

NFR15

## Comparison of Fracture Intensity Measured in Outcrop and $\mu$ CT Core Plugs in a Carbonate Reservoir Analogue

S. Kokkalas<sup>1</sup>, R. Jones<sup>2</sup>, M. Wilkinson<sup>2</sup>, S. Daniels<sup>2</sup>, S. Gilment<sup>2</sup>, S. Nizamuddin

<sup>1</sup> Department of Geology, University of Patras; <sup>2</sup> Geospatial Research, University of Durham;

<sup>3</sup> ADNOC Research & Innovation Center, Khalifa University

### Summary

---

The porosity and permeability structure of fractured reservoirs is highly heterogeneous, however typical sub-surface data are unable to quantify this heterogeneity across scales of analysis that are most relevant for fluid flow. Comprehensive analysis of outcrop analogues can provide detailed, quantitative characterisation of the fracture network to produce robust ranges of values for input to discrete fracture network (DFN) or other fracture models. We compare fracture intensities measured from 3D X-Ray Computed Micro-Tomography with those calculated from scan lines measured along 1D tape measure transects in outcrop, and from multiple virtual scan lines in 3D point cloud data acquired from terrestrial laser scanning (lidar) and digital photogrammetry. Micro-tomography is also useful to help extend understanding of fracture intensities to analysis of fracture porosity.

## Introduction

Most natural fractured carbonate reservoirs display widely varying fracture network characteristics, including fracture size, intensity, density, orientation, clustering and connectivity. This high degree of heterogeneity can have a significant impact on reservoir quality and production. Outcrop analogues can provide invaluable information on the fracture-controlled behaviour of carbonate facies and are key elements in the understanding of reservoir architecture and heterogeneity (Jones et al., 2015). Subsurface data are typically too sparse, directionally biased, and/or too low resolution to capture and quantify the representative heterogeneity of a full fracture network. This often leads to misinterpretation of well data and poor reservoir modelling. Outcrop analogue studies can significantly improve the understanding of fracture characteristics and their impact on fluid flow in hydrocarbon reservoirs.

Characterisation of the natural fracture network is also important for stimulated reservoirs. Novel models attempt to use an integrated approach to consider fracture stages (i.e. hydraulic fracturing) with different fracture intensities in a stimulated reservoir volume (SRV) consistent with observations in the field. Fracturing of horizontal wells in tight reservoirs not only form new fracture volume around the well but also reactivate natural fractures to some extent, which is vital to production (Yuan et al., 2015).

In this presentation we apply a strategy of capturing fracture data across multiple scales, combining laboratory-based micro-tomography, traditional fieldwork, and digital 3D data capture in a key outcrop along the Cretaceous Wasia and Thamama Group contact, in Ras Al-Khaimah, UAE (Fig. 1).

## Methods

Modern methods of digital acquisition, including terrestrial lidar and photogrammetry, are particularly adept at capturing detailed geometrical and geospatial attributes over wide areas. Their main advantage is that they result in more robust datasets over a larger scale-range, particularly for fracture heights, lengths, spacing, clustering, termination and connectivity. The acquired 3D point clouds were used to extract detailed fracture networks from the studied outcrop, including fracture orientations and 1D fracture density along two ~180 m long scanlines. Further details of the technical parameters used for the lidar and photogrammetric studies of this outcrop are given in Wilkinson et al. 2016.



**Figure 1** Lidar scanning of Wasia and Thamama carbonates at Ras Al-Khaimah.

To analyse fracture characteristics at microscopic scale, large rock samples were collected along these two scanlines, and standard plug-sized samples (1.5" diameter x ca. 3" length [3.8cm x ~7.6cm]) were drilled along three orientations orthogonal to each other, with one plug normal to the bedding and two along the bedding and orthogonal to each other (Fig. 2). The core-plugs were analyzed using 3D X-Ray Computed Micro-Tomography ( $\mu$ CT), as described in detail by Wennberg et al., 2009. This is a non-destructive technique that records the interior of the sample in high resolution and high contrast, to image the internal 3D fracture geometries (Fig. 2). Numerous sections (e.g. 2000-4200) of the sample are captured precisely in 2D to allow the 3D object to be reconstructed.

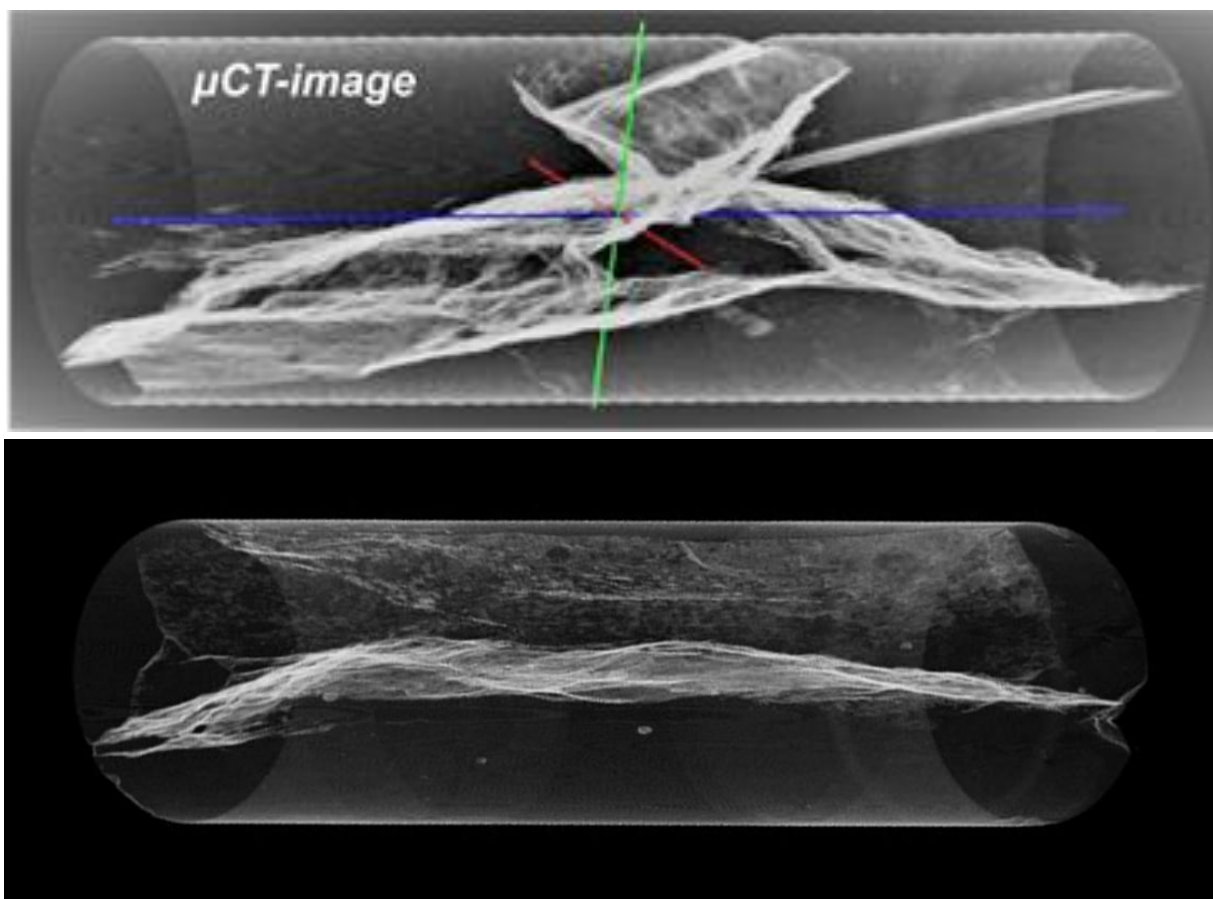


**Figure 2** Examples of high resolution micro-CT images from the examined core plugs, showing the detailed geometry of overlapping microfractures. Diameter of core plugs = 3.6cm

The plug-size samples were scanned using a Zeiss Xradia-520 Versa instrument, available with a maximum 160 kV high-energy and micro-focused X-ray tube. The device is equipped with a 2048 x 2048 pixels, noise suppressed, charge coupled detector assembly, with an innovative dual-stage system for acquiring high contrast images. For all samples, between 2651 and 4601 projections were taken. The distance of source and detector from the sample was chosen to be 73 mm and 50 mm respectively, resulting in a voxel size of 40.39 microns. After scanning, the data were reconstructed (i.e. a 3D image created from all the 2D radiogram projections) using the software included with the instrument.

In order to obtain features from the 2D images we applied a simple binary segmentation, by recording the range of pixel intensity values that represent the fractures in all slices of the sample. In order to better visualize the fractures in the 2D slice, a MATLAB code was written to segment the pixel intensity values that represent the fractures and assign those pixels white colouring, while the remaining pixels of the matrix in the slice are coloured black. All the segmented slices were loaded in VolView software (open source, [www.kitware.com/volview/](http://www.kitware.com/volview/)), to visualize the segmented slices in 3D. This 3D view showed the fracture network distribution inside the samples in great detail (Fig. 2).

## 1D, 2D and 3D Fracture Intensities

Estimating the 3D volumetric fracture intensity ( $P_{32}$ ) is a challenging task and most often is estimated indirectly from the 1D  $P_{10}$  or 2D  $P_{21}$  fracture intensity (Wang, 2005). The 3D fracture intensity ( $P_{32}$ ) can be expressed as the area of fracture per unit volume of rock mass (Singhal and Gupta, 2010):

$$P_{32} \text{ fracture intensity (m}^{-1}\text{)} = \text{fracture surface area (m}^2\text{)} / \text{sample volume (m}^3\text{)}.$$

Tomography analysis provides a direct measure of  $P_{32}$  fracture intensity. The fracture surface area is determined by counting the voxels in the complex fracture network in all slices of the sample, and multiplying the number of voxels by the pixel size to get the surface area of the fractures ( $\text{m}^2$ ). This area is divided by the sample volume ( $\text{m}^3$ ) to obtain the fracture density of the sample (in  $\text{m}^{-1}$ ). The 1D scanlines measured along tape measure transects in outcrop gave  $P_{10}$  intensities that we converted to  $P_{32}$  intensities using the Wang method. Similarly, for 3D point cloud data from lidar and/or photogrammetry, we created multiple closely-spaced 1D virtual scanlines along the outcrop, and converted intensities from  $P_{10}$  to  $P_{32}$ .

## Results: 3D Fracture Intensity

All estimates of fracture intensity are scale-dependant, and will under-estimate the contribution to total fracture intensity of fractures with sizes below the detection threshold for a given acquisition method. The  $P_{32}$  fracture intensities calculated from various scales and resolutions ranges from  $0.75\text{-}3 \text{ m}^{-1}$  from lidar and photogrammetry ( $P_{10} \rightarrow P_{32}$ ),  $9\text{-}20 \text{ m}^{-1}$  from field measurements ( $P_{10} \rightarrow P_{32}$ ), to  $12\text{-}160 \text{ m}^{-1}$  (with an average  $P_{32}$  value of  $33.5 \text{ m}^{-1}$ ) from  $\mu\text{CT}$  data. It is important to note that the  $P_{32}$  fracture intensity obtained by  $\mu\text{CT}$  is expected to be much higher than the calculated values from other techniques, since this method is highly sensitive to distinct fracture orientation and size distribution, as well as due to the higher level of detail available in the  $\mu\text{CT}$  scan. This is also the underlying reason why it generally represents an appropriate estimate of background fracture intensity to use in the context of DFN modelling.

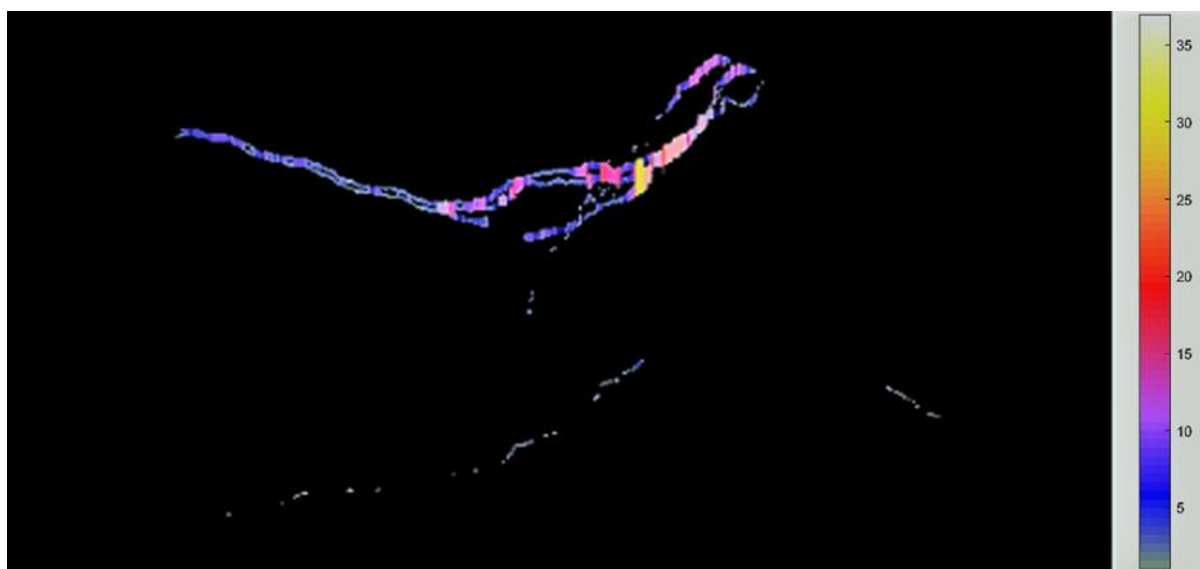


**Figure 3** Aperture variation along a slice of a mCT-image (coloured scale in voxels: 1 voxel =  $40.3\mu\text{m}$ ).

## Discussion: 3D Fracture Porosity

For dynamic flow modelling of fractured reservoirs we need to extend our analysis of  $P_{32}$  fracture intensities to consider  $P_{33}$  fracture porosities. This requires a better understanding of fracture apertures, including the spatial distribution of aperture heterogeneities. In the micro-CT analyses, the

aperture width clearly varies along the fractures (Fig. 3), implying that it is meaningless to assign a single aperture value for fractures in reservoir models. Therefore, an aperture width distribution over the 2D slice or along the full sample would be ideal. In this study, we calculated aperture width by measuring the distance normal to the fracture walls; i.e. by measuring the number of pixels lying between the two fracture walls. The full slice aperture distribution is displayed with a colour scale in Fig. 3 and by multiplying the aperture distribution with the micro-CT scan resolution, we can obtain the fracture aperture in  $\mu\text{m}$  or  $\text{mm}$ . In Fig.3, from one of our most fractured samples, the fracture aperture ranges from 0.2-0.6 mm, with a maximum value of around 1.2 mm often located in the overlap zone or relay zone formed between individual fracture segments.

Measured total porosity was low in the plug-size samples obtained from outcrop, ranging from 0.21 to 2.5%, indicating that fracture porosity plays a major role in the tight carbonates of the Wasia Fm. The actual fracture porosity values ( $P_{33}$ ) of the plug-size samples, measured using the total fracture volume over the bulk sample volume, displays a range from 0.17-1.2%.

## Conclusions

The described pilot-study applied an integrated microstructural and outcrop methodology to a reservoir analogue to provide high resolution inputs for reservoir geo-modelling workflows. The resultant digital 3-D analogue, from outcrop scale to core plug scale, provides key data for the spatial representation of heterogeneities that illustrate the complexity of fractured-carbonate reservoirs. Fracture parameters quantified across a wide range of scales, and combined with elastic mechanical properties of the carbonate layers, represent an ideal basis for the calibration of multi-scale fractured reservoir models.

## Acknowledgements

We thank the ADNOC Research and Innovation Centre for permission to use the  $\mu\text{CT}$  equipment.

## References

- Daniels, S., Imber, J., Jones, R., Long, J., Kokkalas, S., 2015. How can fracture studies of outcrop analogues inform geomechanics? Geology of Geomechanics conference. Geological Society of London, October 2015.
- Jones, R.R., Long, J.J., Kokkalas, S., Daniels, S.E., Oxlade, D.M., Gilment, S.R., Woods, C.E., Wilkinson, M.W., 2015. Improved Multi-Scale Fracture Models Based on Quantitative Analysis of Outcrop Analogues. Third EAGE Workshop on Iraq. DOI: 10.3997/2214-4609.201414364
- Singhal, B.B.S., Gupta, R.P., 2010. Applied Hydrogeology of Fractured Rocks, 2<sup>nd</sup> ed. Springer Science & Business Media B.V.
- Wang, X., 2005. Stereological interpretation of rock fracture traces on borehole walls and other cylindrical surfaces. Ph.d., Virginia Polytechnic Institute and State University.
- Wennberg, O.P., Rennan, L., Basquet, R., 2009. Computed tomography scan imaging of natural open fractures in a porous rock; geometry and fluid flow. Geophysical Prospecting, 57, 239–249. DOI: 10.1111/j.1365-2478.2009.00784.x.
- Wilkinson, M.W., Jones, R.R., Woods, C.E., Gilment, S.R., McCaffrey, K.J.W., Kokkalas, S.K., Long, J.J., 2016. A comparison of terrestrial laser scanning and structure-from-motion photogrammetry as methods for digital outcrop acquisition. Geosphere, 12, DOI: 10.1130/GES01342.1
- Yuan, B., Su, Y.L., Moghanloo, R.G., Rui, Z., Wang, W., Shang, Y., 2015. A new analytical multi-linear solution for gas flow toward fractured horizontal wells with different fracture intensity. Journal of Natural Gas Science and Engineering, 23, 227–238.